

Discrete-time quadrature feedback cooling of a radio-frequency mechanical resonator

M. Poot*,¹ S. Etaki,^{1,2} H. Yamaguchi,² and H. S. J. van der Zant^{1,†}

¹*Kavli Institute of Nanoscience, Delft University of Technology, Lorentzweg 1, 2628 CJ Delft, The Netherlands*

²*NTT Basic Research Laboratories, NTT Corporation, Atsugi-shi, Kanagawa 243-0198, Japan*

(Dated: September 11, 2018)

We have employed a feedback cooling scheme, which combines high-frequency mixing with digital signal processing. The frequency and damping rate of a 2 MHz micromechanical resonator embedded in a dc SQUID are adjusted with the feedback, and active cooling to a temperature of 14.3 mK is demonstrated. This technique can be applied to GHz resonators and allows for flexible control strategies.

Mechanical systems in the quantum regime [1–3] can be used to answer fundamental questions about quantum measurement, decoherence, and the validity of quantum mechanics in macroscopic objects. This requires a mechanical resonator which is cooled to such a low temperature that it is in its ground state for most of the time. In the past few years tremendous progress has been made in actively cooling resonators [3], mainly by using sideband cooling [2, 4, 5] and active feedback cooling [6–8]. The latter technique has mainly been applied to low-frequency (kHz) resonators combined with optical detection. The largest cooling factors have been obtained using velocity-proportional feedback, i.e., by feeding back the differentiated displacement signal. However, at higher frequencies, delays in the feedback system seriously degrade the cooling performance. Here, we demonstrate a feedback cooling technique [9] with a nearly unlimited bandwidth, based on fast digital signal processing (DSP) in combination with single-sideband mixing. A 2 MHz micromechanical resonator with inductive readout is cooled to 14.3 mK using this scheme.

Figure 1a shows the device, which consists of a dc SQUID with a part of its loop suspended. This forms a 50 μm long flexural resonator with its fundamental mode around $f_0 \sim 2$ MHz. The chip is glued onto a piezo element for feedback and actuation, and cooled in a dilution refrigerator with a minimum bath temperature of 15 mK. By applying an in-plane magnetic field B (green), a displacement of the beam u changes the amount of flux through the dc SQUID loop. When a bias current I_B is applied, a change in flux results in a change in the SQUID voltage V . This way, the dc SQUID is a sensitive displacement detector [10]. In all measurements presented here, the same working point for the dc SQUID is used, to avoid backaction-induced changes in frequency and damping [11].

The thermal noise of the resonator is used to calibrate the dc SQUID detector. Figure 1b shows the displacement noise spectrum S_{uu} measured at two different cryostat temperatures T . The thermal motion of the res-

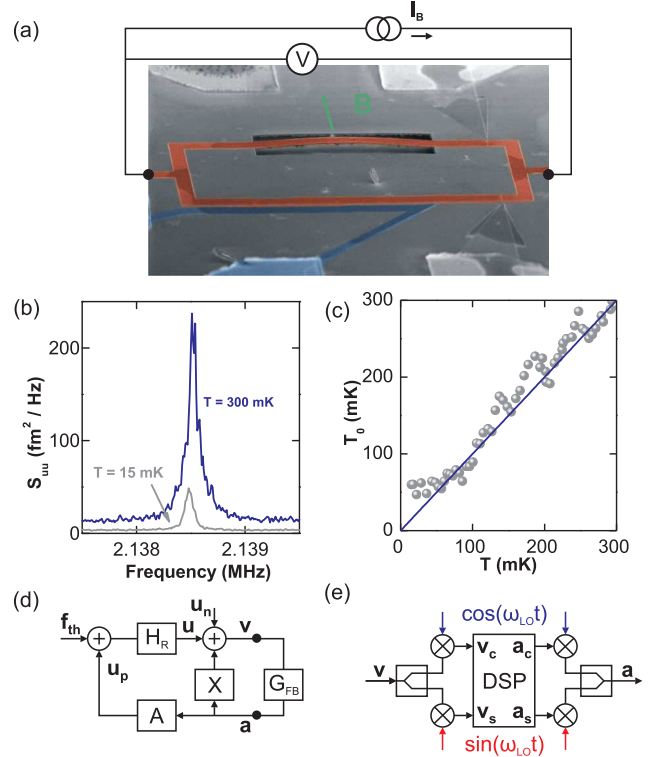


FIG. 1: (a) Schematic overview of the SQUID detector (red) with the integrated flexural resonator. (b) Displacement noise spectra without feedback. (c) The resonator temperature extracted from the thermal noise spectra plotted against the mixing chamber temperature. (d) Generic linear system representation [12] of feedback cooling. (e) The feedback filter consists of a digital signal processor with a single-sideband mixer at the input and output.

onator shows up as a peak on top of the imprecision noise floor $S_{u_n u_n}$. The cryogenic-amplifier-limited displacement noise is $2 \text{ fm}/\sqrt{\text{Hz}}$ at $T = 15$ mK. The area under the peak is the amplitude of the Brownian motion of the resonator squared. When the temperature of the refrigerator is increased to $T = 0.3$ K, the spectrum changes: Firstly, the noise floor is higher due to a decrease in the transduction, dV/du , as the critical current decreases with increasing temperature [10]. Secondly, the peak is higher and wider (the intrinsic damping rate γ_0

*Present address: Department of Electrical Engineering, Yale University, New Haven, CT 06520, USA

†Electronic address: h.s.j.vanderzant@tudelft.nl

increases with temperature), indicating that the thermal motion is larger at higher temperatures. The resonator temperature $T_0 = k_0 \langle u^2 \rangle / k_B$ ($k_0 = 110$ N/m is the spring constant) is plotted against T in Fig. 1c: It follows the cryostat temperature for $T > 50$ mK (solid line) and saturates below this value.

To further lower the resonator temperature, active feedback is employed, where the displacement of the resonator is fed back to it to damp its thermal motion. Fig. 1d illustrates the generic process [3]: The thermal force noise $F_{th} \equiv k_0 f_{th}$ drives the resonator whose response is $H_R = f_0^2 / (f_0^2 - f^2 + if\gamma_0/2\pi)$. Note, that f_{th} and the other signals are scaled to have the unit of position. The force results in a displacement which is measured by the dc SQUID detector, and imprecision noise u_n is added to its output v . This signal is fed to the feedback filter with transfer function G_{fb} . The actuation a is multiplied by A , which consists of the SQUID transduction, an attenuation (-40 dB) and the piezo responsivity. Finally, the resulting piezo displacement u_p exerts an inertial force on the resonator. Note, that in practise crosstalk (X) exists between the applied feedback and the detector output, which modifies the system response.

To fully characterize the linear system an ac signal is applied to a (see Fig. 1d) and the response at v is measured at the same frequency, while sweeping the driving frequency across the resonance. In this case, the feedback G_{fb} is disabled. From this network-analyzer measurements the elements $A = 1.94 \cdot 10^{-4} \exp(-0.73i)$, and $X = 0.26 \exp(2.56i)$ of the linear systems are obtained as well as the parameters of H_R : f_0 and γ_0 . The non-zero phase of A is due to the time it takes for the signal to travel through the whole system. If an analog differentiator would be used for G_{fb} , this delay causes the feedback to not be purely velocity proportional thus degrading the cooling performance. The DSP-based feedback presented here can compensate for this effect as demonstrated below.

Our implementation of the feedback filter G_{fb} is shown in Fig. 1e. The high-frequency input signal v is split and both branches are mixed with local oscillator (LO) signals with a 90° phase difference between them. This IQ mixer gives both quadratures v_s and v_c of the input signal. The LO frequency is $f_{LO} = 2.0492$ MHz so the down-mixed signals oscillate at $f_R - f_{LO} = 8.9$ kHz. They are digitized and the DSP (Adwin Pro II at a sampling rate $f_s = 820$ kS/s) applies the following transformation to the input signals to generate two output signals a_c and a_s :

$$\begin{pmatrix} a_c \\ a_s \end{pmatrix} = g_{fb} \begin{pmatrix} \cos \theta_{fb} & -\sin \theta_{fb} \\ \sin \theta_{fb} & \cos \theta_{fb} \end{pmatrix} \begin{pmatrix} v_c \\ v_s \end{pmatrix} \quad (1)$$

These quadratures are then up-converted by the LO frequency with a second IQ mixer. The final result is a signal a at the original frequency that is phase-shifted by the feedback phase θ_{fb} and multiplied by the feedback gain g_{fb} , i.e. $G_{fb} = g_{fb} \exp(i\theta_{fb})$. The only frequency requirement for this mixing scheme is that the quadratures do not change faster than the sampling rate, which is equivalent to $\gamma_R/2\pi \lesssim f_s/2$. The operation is thus not limited to resonators with frequencies within the bandwidth of the DSP, allowing feedback cooling of radio and microwave frequency resonators. Note, that the imprecision noise floor is still determined by the cryogenic amplifier; the contributions from the mixers and discretization are negligible.

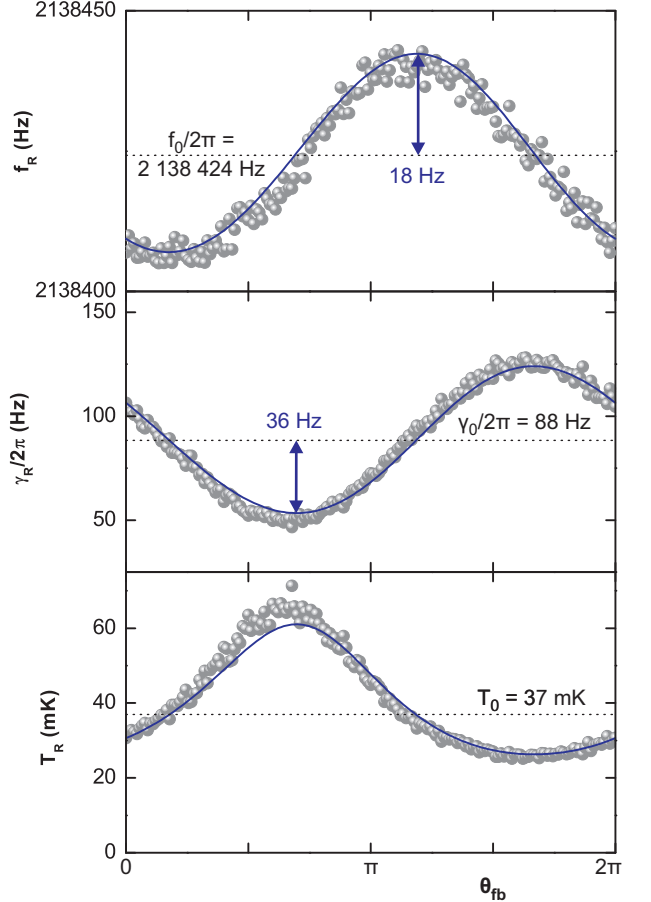


FIG. 2: Feedback phase dependence of the resonator frequency (a), damping rate (b), and resonator temperature (c) for $g_{fb} = 0.1$. The dashed lines indicate their measured values in the absence of feedback, (f_0 , γ_0 , and T_0 resp.); the solid line is the phase dependence calculated using independent measurements.

The feedback modifies the resonator response from H_R to its closed-loop form H'_R [3]:

$$H'_R = \frac{f_0^2}{f_0^2 - f^2 + if\gamma_0/2\pi - f_0^2 G'_{fb} A}, \quad (2)$$

where $G'_{fb} = g'_{fb} \exp(i\theta'_{fb}) = G_{fb}/(1 - XG_{fb})$ is the feedback filter modified by the crosstalk. The real part of $G'_{fb} A$ modifies the resonance frequency from f_0 to $f_R \approx f_0(1 - \text{Re}[G'_{fb} A]/2)$, whereas the imaginary part changes the damping from γ_0 to $\gamma_R \approx \gamma_0 - 2\pi f_0 \text{Im}[G'_{fb} A]$. Both the frequency shift and the change in damping de-

pend periodically on the phase of $G'_{fb}A$ and the maximum frequency shift is half the maximum damping rate change.

In order to achieve optimal cooling the feedback phase is varied for a fixed feedback gain as shown in Fig. 2. The feedback gain is chosen sufficiently small so that $G'_{fb} \approx G_{fb}$. At every point the thermal noise spectra are measured and fitted to obtain the resonance frequency (top), the damping rate (center), and the resonator temperature (bottom). The resonance frequency and damping rate show the expected sinusoidal dependence on the feedback phase. The amplitude of the frequency shift is half of that of the change in damping, consistent with the discussion above. The phase where the damping is maximized, coincides with the lowest resonator temperature and zero frequency shift. At this phase the system delay is compensated and a pure velocity-proportional feedback is applied to the resonator (i.e. $\angle AG_{fb} = -\pi/2$). The phase dependencies can also be calculated without any free parameters by using the values from the network characterization (Fig. 1d). Figure 2 show that these are in good agreement with the feedback results.

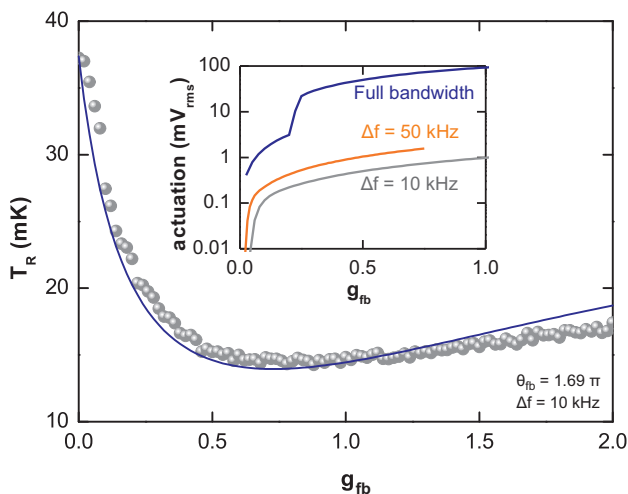


FIG. 3: Resonator temperature as a function of feedback gain, showing both the feedback measurements (symbols) and calculations for pure velocity-proportional feedback (solid line). The inset shows the root-mean-squared value of the actuation signal ($\sqrt{\langle a_c^2 \rangle + \langle a_s^2 \rangle}$) as a function of gain for different filter bandwidths.

To further cool the resonator, the feedback gain is increased at the optimal phase as indicated in Fig. 3. First the resonator temperature decreases rapidly with increasing gain due to the increased damping rate. However, by increasing the gain further, more of the imprecision noise u_n is fed back as force noise. This causes a steady increase in T_R for large g_{fb} . The minimum temperature that can be reached is set by $S_{u_n u_n}$ and the solid line shows the predicted curve for velocity-proportional feedback [7, 13] calculated with the experimental parameters. The achieved minimum of 14.3 mK is close to the predicted lowest temperature of 14.0 mK. Note, that a temperature of 14.3 mK corresponds to an average thermal phonon occupation of $\bar{n} \approx k_B T_R / h f_R = 138$ for a 2 MHz resonator. The heterodyne DSP-based technique employed in this work thus successfully reaches the lowest temperature possible for the standard fully-analog approach, but now applied to a high-frequency resonator.

Another advantage of DSP-based feedback is that the transformation of v_s and v_c to a_c and a_s can be designed with almost arbitrary transfer characteristics, allowing implementation of optimal control strategies [14]. In the measurements in Fig. 3, the input signal is digitally filtered using a Fourier transform filter which is centered around f_0 and a tunable filter bandwidth Δf . The filter reduces the bandwidth of the feedback which prevents excess signal output outside the resonator bandwidth that may overload the detector or the amplifiers. The inset of Fig. 3 shows the root-mean-square output voltage as a function of g_{fb} for three values of Δf . For the full bandwidth ($f_s/2 = 410$ kHz) an instability occurs around $g_{fb} = 0.23$, which affects the cooling. The 10 kHz bandwidth, which is used for the cooling curve of Fig. 3, has two orders of magnitude less actuation compared to the full bandwidth, enabling efficient cooling without affecting the closed-loop response as long as $\Delta f \gg \gamma_R/2\pi$. This again illustrates the versatility of our digital quadrature feedback cooling platform.

We thank Hidde Westra, Khasahir Babei Gavan, Abah Obinna and Joris van der Spek for their help with the measurements. This work was supported in part by FOM, NWO (VICI grant), NanoNed, a EU FP7 STREP project (QNEMS), and JSPS KAKENHI (20246064 and 23241046).

-
- [1] A. D. O’Connell, M. Hofheinz, M. Ansmann, R. C. Bialczak, M. Lenander, E. Lucero, M. Neeley, D. Sank, H. Wang, M. Weides, et al., *Quantum ground state and single-phonon control of a mechanical resonator*, Nature **464**, 697 (2010).
- [2] J. D. Teufel, T. Donner, D. Li, J. H. Harlow, M. S. Allman, K. Cicak, A. J. Sirois, J. D. Whittaker, K. W. Lehnert, and R. W. Simmonds, *Sideband cooling mi-*

cromechanical motion to the quantum ground state, arXiv:1103.2144v1 (2011).

- [3] M. Poot and H. S. J. van der Zant, *Mechanical systems in the quantum regime*, Phys. Rep., submitted (2011).
- [4] O. Arcizet, P.-F. Cohadon, T. Briant, M. Pinard, and A. Heidmann, *Radiation-pressure cooling and optomechanical instability of a micromirror*, Nature **444**, 71 (2006).

- [5] T. Rocheleau, T. Ndukum, C. Macklin, J. B. Hertzberg, A. A. Clerk, and K. C. Schwab, *Preparation and detection of a mechanical resonator near the ground state of motion*, Nature **463**, 72 (2010).
- [6] D. Kleckner and D. Bouwmeester, *Sub-kelvin optical cooling of a micromechanical resonator*, Nature **444**, 75 (2006).
- [7] M. Poggio, C. L. Degen, H. J. Mamin, and D. Rugar, *Feedback Cooling of a Cantilever's Fundamental Mode below 5 mK*, Phys. Rev. Lett. **99**, 017201 (pages 4) (2007).
- [8] B. A. *et al.*, *Observation of a kilogram-scale oscillator near its quantum ground state*, New J. Phys. **11**, 073032 (2009).
- [9] T. E. Kriewall, J. L. Garbini, J. A. Sidles, and J. P. Jacky, *Heterodyne Digital Control of a High-Frequency Micromechanical Oscillator*, Journal of Dynamic Systems, Measurement, and Control **128**, 577 (2006).
- [10] S. Etaki, M. Poot, I. Mahboob, K. Onomitsu, H. Yamaguchi, and H. S. J. van der Zant, *Motion detection of a micromechanical resonator embedded in a d.c. SQUID*, Nat Phys **4**, 785 (2008).
- [11] M. Poot, S. Etaki, I. Mahboob, K. Onomitsu, H. Yamaguchi, Y. M. Blanter, and H. S. J. van der Zant, *Tunable Backaction of a DC SQUID on an Integrated Micromechanical Resonator*, Phys. Rev. Lett. **105**, 207203 (2010).
- [12] A. V. Oppenheim, A. S. Willsky, and S. Hamid, *Signals and Systems*, Prentice Hall signal processing series (Prentice Hall, Englewood Cliffs, NJ, 1997), 2nd ed.
- [13] K. H. Lee, T. G. McRae, G. I. Harris, J. Knittel, and W. P. Bowen, *Cooling and Control of a Cavity Opto-electromechanical System*, Phys. Rev. Lett. **104**, 123604 (2010).
- [14] K. J. Bruland, J. L. Garbini, W. M. Dougherty, and J. A. Sidles, *Optimal control of force microscope cantilevers. II. Magnetic coupling implementation*, J. Appl. Phys. **80**, 1959 (1996).